Statics and Dynamics of Polymer-Wrapped Colloids†

N. Bagatella-Flores,‡ H. Schiessel,*,§ and W. M. Gelbart‖

Facultad de Física e Inteligencia Artificial, Universidad Veracruzana, Xalapa, Veracruz, Mexico, Instituut-Lorentz, Universiteit Leiden, P.O. Box 9506, 2300 RA Leiden, The Netherlands, and Department of Chemistry and Biochemistry, University of California, Los Angeles, California 90095

Received: June 7, 2005; In Final Form: August 18, 2005

We study the complex between a colloidal particle and a semiflexible polymer chain that "wraps" around it. Via molecular dynamics simulation we investigate statistical and dynamical properties of this system. First we establish the dependence of wrapped chain length on absorption energy and chain persistence length and obtain the distribution of wrapped-sphere positions. Then we study the length and position distributions of thermally excited loop defects. Finally we consider the repositioning dynamics of the colloid, focusing on the case where the chain stays wrapped onto the complex. Specifically we determine the mean square displacement of the central monomer of the wrapped chain and the resulting diffusion coefficient of the chain as a function of its persistence length, absorption energy, chain length, and size of the sphere. We argue that both statics and dynamics of these complexes can be mainly understood by energetic arguments, whereas entropic contributions from the chain configurations play only a minor role.

I. Introduction

The stability and the aggregation behavior of colloidal suspensions in nonpolar solvents can be controlled by synthetic neutral polymers.[1] In aqueous solutions, charged polymers (polyelectrolytes) play a similar role.[2] Particularly interesting examples are found in living cells where charged biopolymers such as DNA interact with macroions, e.g., proteins. Most prominently, the complexation of DNA with histone proteins is the basis for the reversible coordinated condensation of long eukaryotic DNA strands of the order of centimeters into the highly compacted chromatin complex that is confined in the micron-size nucleus.[3] At the lowest point of the hierarchy of this condensation process, DNA strands are wrapped around cylindrical histone octamers that carry a charge opposite to that of DNA.

Systems of colloidal particles and polymers show a rather complex phase behavior, cf., for instance, ref 4. The problem simplifies significantly if one considers model systems that consist of one chain and one sphere only. We will focus here on the case of a semiflexible chain (such as DNA) where the persistence length is of the order of or larger than the particle size (for the case of flexible chains cf. ref 5). This problem was first treated by Marky and Manning[6] who studied the complexation between a disklike particle and a chain due to short-range attraction. They found that this system can be either in a bound state where the chain wraps around the particle or in a dissociated state. By changing the binding energy or the persistence length of the chain one can induce an abrupt transition from the bound to the free state.

More recent theoretical studies have refined this picture in mainly three directions. (*i*) The electrostatics of such systems was explicitly included, i.e., the complex is made from a charged chain and an oppositely charged sphere. What all these studies have in common is that they feature the phenomenon of "overcharging", i.e., the charge of the wrapped chain portion typically overcompensates the colloidal charge.[7−12] (*ii*) The unwrapping of chains (upon a change of parameters) was investigated in detail and it was demonstrated that there exist a multitude of more open complexes, including partially wrapped states[13,14] and rosette configurations.[3,15−20] (*iii*) The dynamics of the sphere diffusion *along* the chain has been studied; this, however, exclusively in the context of nucleosomes.[3,21−26]

In the present work we investigate static and dynamic properties of polymer−colloid complexes using molecular dynamics (MD) simulations. We study complexes where a semiflexible polymer is wrapped onto a "sticky" colloid. We especially focus on the dynamics of the colloid, namely its repositioning along the chain, and aim at elucidating the underlying mechanism. Before doing so, we first study related problems of the statics of the complex, especially the positioning of the colloid along the chain and the occurrence of loop defects. As we shall show, the statics of this complex is governed by different mechanisms than that of a system where a polymer and a colloid are attracted via a long-range electrostatic interaction.[7−12] Also, the repositioning dynamics of our polymer-wrapped colloid that is based on the smoothness of the colloid surface contrasts sharply to nucleosome repositioning along DNA, where the discreteness of the binding site is crucial for its dynamics.[25,26]

The paper is organized as follows. In section II we present our model system in detail. It consists of a semiflexible chain and a spherical colloid that interact via a short-ranged potential. Section III is devoted to an investigation of equilibrium properties of the wrapped complex, especially to the question of the distribution of the sphere position along the chain. In section IV we consider "imperfectly" wrapped states that contain loop defects. Section V presents results concerning the diffusion of the sphere along the chain. We study the influence of parameters such as the ball-chain interaction strength or the chain stiffness on the relative mobility between the two constituents of the complex. In the final section we provide a conclusion and discussion.

† Part of the special issue "Irwin Oppenheim Festschrift".
‡ Universidad Veracruzana.
* To whom correspondence should be addressed.
§ Universiteit Leiden.
‖ University of California, Los Angeles.

10.1021/jp053023e CCC: $30.25
Published on Web 09/29/2005

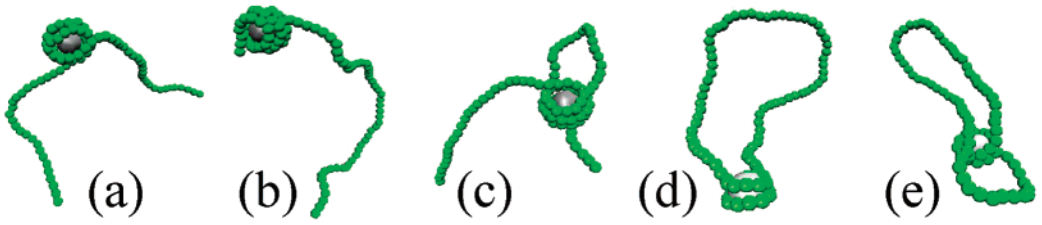

Figure 1. Example configurations of the sphere−chain complex for two different situations: Cases a−c correspond to a wrapped chain with two free ends while d and e show chains whose ends are closed into a ring.

II. Model and Methods

This section presents our model of a polymer−colloid complex. The colloid is modeled as a sphere of radius R. The polymer is a semiflexible chain made from N monomers (i = 1 to N) of size σ with an overall chain length $L = \sigma N$. The chain stiffness is characterized by a persistence length l_p. We assume a short-ranged attraction between the sphere and the chain with a strength k^a per monomer. The conformation of the chain is given by the set $\{\vec{r}_i\}$, with $\vec{r}_i$ being the position of monomer i. We denote the position of the center of the colloid by $\vec{r}_s$. Example configurations of such complexes are depicted in Figure 1.

The energy of each monomer is a sum of four contributions:

$$u^{\text{total}}(\vec{r}_i) = u^{\text{stretch}} + u^{\text{bend}} + \sum_{j\neq i} u^{\text{LJ}} + u^{\text{adsorb}} \tag{1}$$

The first term accounts for the connectivity between nearest neighbors that we model via a harmonic stretching potential

$$\beta u^{\text{stretch}}(\vec{r}_{i-1},\vec{r}_i,\vec{r}_{i+1}) = \frac{k^s}{2\sigma^2}[(|\vec{r}_i - \vec{r}_{i-1}| - \sigma)^2 + (|\vec{r}_{i+1} - \vec{r}_i| - \sigma)^2] \tag{2}$$

where $\beta = 1/k_BT$ and k^s denotes the dimensionless spring constant; we choose $k^s = 400$ in the following. We will consider mostly open chains, cf. Figures 1a to c. In section V we close the chain into a ring as in Figures 1d and e; this will turn out to be a convenient means to measure the dynamics of the sphere along the chain. The flexibility of the chain enters through a bending potential between neighboring monomers

$$\beta u^{\text{bend}}(\vec{r}_{i-1},\vec{r}_i,\vec{r}_{i+1}) = \frac{k^b\theta^2}{2} \tag{3}$$

where k^b is the dimensionless bending constant, θ is the complementary angle between the vectors $\vec{r}_i(t) - \vec{r}_{i-1}(t)$, and $\vec{r}_{i+1}(t) - \vec{r}_i(t)$. The bending constant is directly related to the chain persistence length via $l_p = \sigma k^b$.

The third term in eq 1 accounts for the excluded volume between any given pair of monomers i and j through a shifted, purely repulsive Lennard-Jones potential

$$\beta u^{\text{LJ}}(r_{i,j}) = 4\epsilon\left[\left(\frac{\sigma}{r_{i,j}}\right)^{12} - \left(\frac{\sigma}{r_{i,j}}\right)^{6} + \frac{1}{4}\right] \tag{4}$$

for $r_{i,j} < 2^{1/6}\sigma$ and 0 otherwise. ϵ denotes the dimensionless Lennard-Jones constant, and $r_{i,j} = |\vec{r}_i - \vec{r}_j|$. Finally, the short-range attraction of monomer i to the impenetrable sphere is taken into account via a Morse potential:

$$\beta u^{\text{adsorb}}(r_i) = k^a[\exp(-2\alpha(r_i - \rho)) - 2\exp(-\alpha(r_i - \rho))] \tag{5}$$

where k^a is the dimensionless absorption or binding constant. The parameter α sets the range of the potential; in the following we always choose $\alpha = 6$. $r_i = |\vec{r}_i - \vec{r}_s|$ denotes the distance from monomer i to the center of the sphere. The minimum of the potential is located at distance $\rho = R + \sigma/2$.

From $u^{\text{total}}(\vec{r}_i)$ follows the force $\vec{F}_i = -\vec{\nabla}u^{\text{total}}(\vec{r}_i)$ that is exerted on monomer i by all the other monomers and by the colloid (neglecting hydrodynamic interactions). This force enters directly into the Langevin equation of the ith particle

$$m\frac{d^2\vec{r}_i}{dt^2} = -\xi\frac{d\vec{r}_i}{dt} + \vec{F}_i + \vec{f}_i, \tag{6}$$

where m is its mass and ξ its friction coefficient. $\vec{f}_i$ is a random thermal noise that mimics the collisions of the ith bead of the chain with the solvent molecules. The thermal noise is Gaussian with zero mean so that $\langle|\vec{f}_i(t)|^2\rangle = 6k_BT\xi/\delta t$, with δt being the time step. Here we choose $\delta t = 0.02$ where the time is measured in units of the Lennard-Jones time $\tau_{LJ} = \sigma\sqrt{m/\epsilon}$.

In most of the following simulations we hold the colloid fixed in space and let only the chain move. In some simulation runs we also allow the colloid to move according to

$$m_s\frac{d^2\vec{r}_s}{dt^2} = -\xi_s\frac{d\vec{r}_s}{dt} + \vec{F}_s + \vec{f}_s \tag{7}$$

We assume that the mass of the colloid m_s is related to the monomer mass m through the ratio of their volumes as $m_s/m = (2R/\sigma)^3$. Furthermore, the friction coefficients of the monomers and the sphere are assumed to follow Stokes' law and are thus related via $\xi_s/\xi = 2R/\sigma$.

III. Static Properties of the Wrapped State

In this section we study the equilibrium properties of the wrapped chain-sphere complex. As can be seen in Figure 1, the chain can either form a wrapped, loop-free structure, cf. Figures 1a and b, or a complex with a loop, cf. Figure 1c. In the current section we will limit ourselves to the subset of configurations without a loop, deferring to the next section all structures where the complex shows a loop.

The N monomers of the chain are distributed between a wrapped section of N_w adsorbed monomers and one or two tails, made from N_{free} monomers: $N = N_w + N_{\text{free}}$. A monomer is defined as being absorbed if its center lies within a distance $R + \delta$ from the center of the sphere where we choose $\delta = \sigma/2$; such monomers experience adsorption energies between $-k^a$ and $-k^a/10$ (see eq 5 with $\alpha = 6$). The number of wrapped monomers depends on several properties of the system: the adsorption and bending energies, k^a and k^b, and the colloid radius R determining the curvature of the wrapped chain section and the total available surface for adsorption on the ball. The other properties, the Lennard-Jones energy ϵ and the bond energy k^s, turn out to have a negligible effect on N_w.

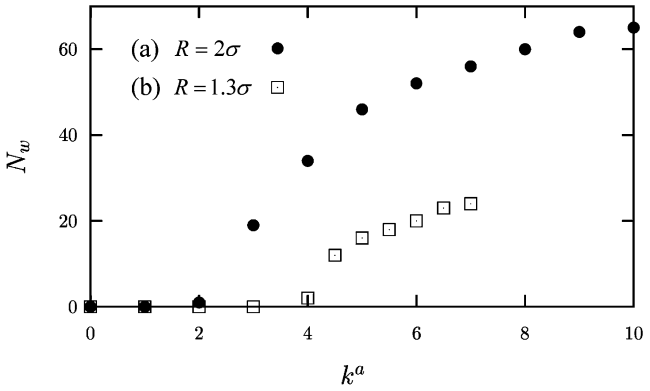

Figure 2. Number N_w of monomers wrapped on the sphere of radius R as a function of the absorption energy k^a for a bending energy constant $k^b = 15$ in two different cases: (a) open chain with $N = 100$ monomers and $R = 2\sigma$ (filled circles), (b) closed chain with $N = 86$ monomers and $R = 1.3\sigma$ (open squares).

In the following we study the number of wrapped monomers N_w as a function of k^a for two different systems. System (a) has a particle radius $R = 2\sigma$ and chain length $N = 100$, and system (b) has $R = 1.3\sigma$ and $N = 86$. In both systems the bending energy is set to $k^b = 15$. We equilibrate the system by making sure that the sphere has visited both ends of the chain several times.

Figure 2 shows the average number of wrapped monomers N_w as a function of k^a. Both cases feature a similar scenario. For small values of k^a there is no adsorption. At a certain threshold, adsorption sets in relatively sharply. Further increase of k^a leads to a further growth of the adsorbed section up to a point where N_w saturates. In both systems the value at saturation is much smaller than the total chain length.

These findings can be rationalized as follows. A chain that wraps onto a ball feels two competing effects: It gains adsorption energy, eq 5, but it pays bending energy, eq 3. Only if the contribution from the attraction outweighs the bending cost, does the chain wrap. This leads to the following condition for wrapping:

$$k^a > k^a_{crit} = \frac{l_p \sigma}{2(R + \sigma/2)^2} = \frac{k^b \sigma^2}{2(R + \sigma/2)^2} \qquad (8)$$

This suggests a wrapping/unwrapping transition at k^a_{crit} in an "all or nothing" fashion as predicted by Marky and Manning.[6] For system (a) we expect this to happen at $k^a_{crit} = 1.2$ and for system (b) at $k^a_{crit} = 2.3$. An inspection of Figure 2 shows a continuous onset of noticeable wrapping at a somewhat larger value of k^a, due to the finite temperature in our simulation. As soon as a wrapped complex has been formed, the amount of wrapped chain rises sharply with k^a.

We consider next the plateau value of N_w for large k^a values. If we forget about the connectivity of the monomers, the number of monomers than can be packed closely in a hexagonal lattice on the surface of the colloid is given by

$$N_{max} = \frac{4\pi(R + \sigma/2)^2}{\sqrt{3}\sigma^2/2} \qquad (9)$$

We find $N_{max} = 90$ for system (a) and $N_{max} = 47$ for system (b), numbers that are significantly larger than the ones that our simulations suggest, cf. Figure 2. Note, however, that the actual maximal number of adsorbed monomers should be expected to be smaller since a perfect hexagonal packing of monomers on the ball cannot be achieved − even for unconnected entities.

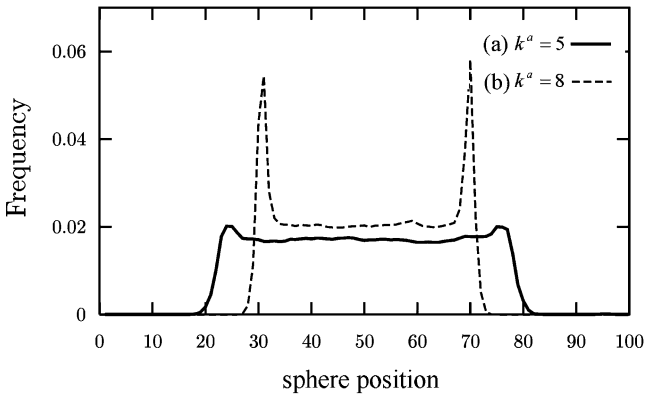

Figure 3. Probability distribution of the sphere position along the chain with $N = 100$, $k^b = 15$, $R = 2\sigma$ for (a) $k^a = 5$ and (b) $k^a = 8$.

Even more importantly, the chain connectivity opposes such a tight packing since it would require sharp bends in the wrapped portion, each bend leading to a large energy penalty.

Equation 8 predicts an "all or nothing" scenario, so one might expect that as soon as the chain starts to wrap it immediately reaches some saturation value. However, as can be seen in Figure 2, the transition is less sharp. This can be explained by the fact that only one turn of the wrapped chain (15 monomers in system (a) and 11 in (b)) can be wrapped with the smallest possible curvature $1/(R + \sigma/2)$. To wrap more than one turn, the chain has to bend considerably more to avoid self-overlap. Therefore, further wrapping is possible only for a larger chain−ball attraction.

Next we study the position of the complexed sphere along the chain. As the snapshots (Figures 1a and b) show, the sphere can be located at either end of the chain, having then all N_{free} monomers located in one arm, or somewhere between so that the complex features two tails. In the following we aim to understand whether there is a preference of the sphere position along the chain. For this purpose we evaluate the probability distribution of that position for several different parameter sets. We characterize the sphere position by the index of the monomer that represents the central monomer of the wrapped portion.

Figure 3 shows the histogram of the sphere positions along the chain for the case where both chain and sphere are allowed to move freely. We compare two cases: (a) weak attraction $k^a = 5$ and (b) strong attraction $k^a = 8$. The other parameters are chosen as follows: $N = 100$, $k^b = 15$, and $R = 2\sigma$. Note that this corresponds to two points in Figure 2, curve (a). As can be deduced from there, the average wrapping length is $N_w = 45$ for $k^a = 5$ and $N_w = 60$ for $k^a = 80$. We find in Figure 3 in both cases a vanishing probability for monomers with indices $i < N_w/2$ and $i > N - N_w/2$, consistent with the fact that, by definition, a chain sitting at one chain terminus has its middle monomer of the wrapped portion at a distance $N_w/2$ from that terminus. The profile of the curve (a) is nearly flat in the "allowed" region $N_w/2 < i < N - N_w/2$, indicating that the sphere has no preferred positions. The situation changes dramatically when one goes to a larger adsorption parameter $k^a = 8$. In this case, the end positions are strongly preferred which manifests itself in peaks of the probability distributions at positions $N_w/2$ and $N - N_w/2$.

This raises the question whether the preferences for end positions that we observed above are caused by energetic or by entropic effects. In first approximation there should not be any energetic dependence of the complexation energy on the ball position. Each adsorbed monomer contributes $-k_BT(k^a - k^a_{crit})$, cf. eq 8, independent of the ball position. In fact, Sakaue

et al.,[22] who also found a strong preference for end positions in their simulation, argue that this effect is of entropic origin.

As we shall see, entropic effects are much too small to explain the strong end preferences found in our Figure 3 and in Figure 2 of ref 22. To show this, we borrow an argument that has been used in the study of translocation of polymers through a pore.[27] This argument overestimates the entropic effect in our system, thereby providing an upper bound for the preference for end positions via an entropic mechanism. Consider a perfectly flexible, ideal (Θ-solvent) chain made from S monomers with one of its ends grafted onto an impenetrable wall. The possible conformations of that chain correspond to three-dimensional random walks that can be decomposed into the directions parallel and perpendicular to the wall. The number of chain configurations in the perpendicular direction can be estimated from the number $\mathcal{N}(S)$ of one-dimensional random walks with S steps that start at the boundary and never return to it: $\mathcal{N}(S) = \sqrt{2/\pi S} \times 2^S$ for $S \gg 1$. The monomer positions in the directions parallel to the wall are not affected by its presence (ideal chain assumption). We make use of this boundary effect to estimate the entropic component of distributing the N_{free} monomers between the two arms of our complex. A tail made from n monomers has a length $n\sigma$ and is thus $S = n/k^{\text{b}}$ persistence lengths long (the fact that the persistence length is much larger than σ allows us here to assume ideal chain statistics). The number of configurations in the symmetric two tail configuration is then estimated as $[\mathcal{N}(N_{\text{free}}/2k^{\text{b}})]^2$ and in the one-tail configuration $\mathcal{N}(N_{\text{free}}/k^{\text{b}})$. This leads to a difference in the free energies

$$\frac{\Delta F}{k_{\text{B}}T} = -\ln\left(\frac{\mathcal{N}^2(N_{\text{free}}/2k^{\text{b}})}{\mathcal{N}(N_{\text{free}}/k^{\text{b}})}\right) = \frac{1}{2}\ln\left(\frac{\pi N_{\text{free}}}{8k^{\text{b}}}\right) \qquad (10)$$

Equation 10 is reliable only for long tails (say 10 l_{p} long). For example for $N_{\text{free}}/k^{\text{b}} = 20$, one finds $\Delta F = 1.0\ k_{\text{B}}T$. This means that an end position is preferred by this amount as compared to the position in the middle. This effect is already very small and becomes all the more so in our case, where we deal with much stiffer chains. In Figure 3 we have $N_{\text{free}}/k^{\text{b}} \approx 4$ for $k^{\text{a}} = 5$ and $N_{\text{free}}/k^{\text{b}} \approx 3$ for $k^{\text{a}} = 8$. In these cases the entropic contribution to the free energy will be much weaker than $k_{\text{B}}T$. Moreover, the free available space is even larger since we have here a finite sized ball instead of an infinite wall (on which our argument was based), i.e., eq 10 overestimates the entropic effect.

This clearly shows that the entropy of the tails cannot explain the strong preference for end positions as found in some of the cases. This is especially so because the chains are so stiff that the bending energy is much too high for a tail to bend back in order to feel the excluded volume of the complex. In fact, the energy of such a tail whose tip touches the complex can be estimated from the energy of a Yamakawa Stockmeyer loop,[28] namely $E_{\text{YS}} = 14.04\ k_{\text{b}}/S$ (S: number of monomers). For the longest tail considered here ($k^{\text{a}} = 5$ in Figure 3) one has $S = 55$, leading already to a bending energy of 4 $k_{\text{B}}T$; in the other cases the energy is even much higher. Most remarkably, however, for the case $k^{\text{a}} = 5$ the preference for end positions is very small whereas the case $k^{\text{a}} = 8$ shows shorter tails *and* a strong preference for end positions. This trend is in contradiction to what one should expect from an entropic argument.

We thus believe that the preference for end positions is enthalpic in origin. As mentioned above, each adsorbed monomer contributes $-k_{\text{B}}T(k^{\text{a}} - k^{\text{a}}_{\text{crit}})$ to the energy. If k^{a} or $R \sim (k^{\text{a}}_{\text{crit}})^{-2}$ is increased, then the effective adsorption energy per monomer increases. The concomitant increase of the occurrence of end positions indicates that for such configurations more monomers can be adsorbed. In fact, if an end monomer is adsorbed on the ball it has more degrees of freedom as compared to a "normal" monomer since it is not connected to tail monomers. A tail monomer connected to an adsorbed monomer might collide with other adsorbed monomers belonging to a nearby winding on the sphere. We speculate that a one-tail complex is able to accommodate roughly one monomer more than one with two tails. This seemingly tiny effect can then easily account for the pronounced peaks in Figure 3 when k^a increases from 5 to 8. The one-tail complex is thus preferred, even though it is here only a tiny effect.

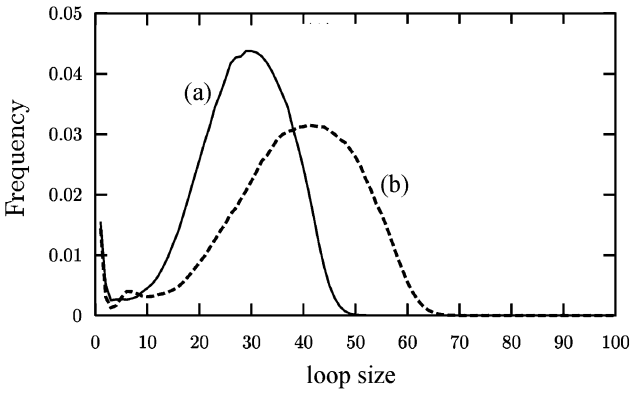

Figure 4. Probability distribution of the loop size with $k^{\text{a}} = 5$ in two cases: (a) $N = 60$, $R = 1.3\sigma$, $k^{\text{b}} = 15$ and (b) $N = 100$, $R = 2\sigma$, $k^{\text{b}} = 20$.

We note that this physical mechanism for end positioning is in sharp contrast to positioning via long-ranged electrostatics. When a charged semiflexible chain is wrapped onto an oppositely charged sphere, the resulting wrapped colloid is either over- or undercharged. An overcharged colloid is repelled from the unwrapped chain portions and hence prefers to be located at one end of the chain (one-tail configuration), whereas an undercharged complex (as arises for stiffer chains) is typically found in the middle of the whole structure surrounded by two tails. Several computer simulations indeed find this effect.[12,14,19] Also, while energetics is responsible here for the positioning, it operates on a much longer length scale and can involve much larger energies.

IV. Static Properties of Complexes with Loops

In the previous section we have restricted ourselves to an analysis of wrapped chain−ball complexes and disregarded configurations where the adsorbed chain forms a loop. Now we study the properties of complexes that show a loop as in the configuration depicted in Figure 1c. We present results on the loop size distribution and on the position of the loop defined as the index of its center monomer, both for several sets of system properties.

We first study the length of a loop that we characterize by the number N_{loop} of its monomers. The monomers of a chain in such a complex can then be divided into three classes: N_{loop} monomers that form the loop, N_{w} wrapped monomers, and N_{free} monomers that are located in the tails. These three numbers add up to the total chain length: $N = N_{\text{w}} + N_{\text{free}} + N_{\text{loop}}$.

Figure 4 presents the distributions of loop sizes for two different cases: (a) $N = 60$ monomers, $k^{\text{a}} = 5$, $R = 1.3\sigma$, and $l_{\text{p}} = 15\sigma$ and (b) $N = 100$ monomers, $k^{\text{a}} = 5$, $R = 2\sigma$, and $l_{\text{p}} = 20\sigma$. In case (a) the probability to find a loop on the complex is $p_{\text{loop}} = 0.18$. When there is no loop, then one has on average

15 adsorbed monomers and 45 free ones (cf. also Figure 2). In the presence of a loop we find a broad distribution of loop sizes with a peak at $N_{loop} = 30$, cf. Figure 4. In case (b) we find a loop with a smaller probability $p_{loop} = 0.13$. Its preferred length is located at $N_{loop} \approx 40$, cf. Figure 4.

These findings can be rationalized by a theory that has been developed to describe loop formation on nucleosomes.[23] The basic idea is that a complex with a loop has a larger free energy than a wrapped complex, mainly due to cost in the bending energy that is stored in the loop. In addition, a complex with a loop is able to accommodate fewer monomers on its surface. The bending energy (in units of k_BT) scales such as l_p/l_{loop} with $l_{loop} = N_{loop}\sigma$ denoting the loop length. Hence small- to medium-sized loops are very costly. When the length of the loop is long enough, namely on the order of the persistence length or longer, the bending energy becomes unimportant and the entropy of the chain configuration, $S = (3/2)\ln(l_{loop}/l_p)$, starts to matter. This means that the free energy has a minimum around $l_{loop} = l_p$, indicating the existence of an optimal loop length for that value. The detailed analysis in ref 23, accounting for the precise loop shapes, shows that this optimal value is actually close to $2l_p$. This is in excellent agreement with the value of the positions of the peaks in Figure 4 for both values of l_p.

Inspecting Figure 4 closely, one finds an additional feature in the loop size distribution, namely an increased probability for very small loops of length $l_{loop} \approx R$ or smaller. This is also found in the exact theory.[23] Small loops of that kind cost mainly desorption but hardly any bending energy. The estimate given above for the bending energy, l_p/l_{loop}, breaks down then due to the finite size of the ball. Such small loops have been studied in ref 21 as possible defect structures on nucleosomes that might induce a repositioning of the octamer along the DNA.

We analyze next the position of the loop along the chain that we characterize by the index of the central loop monomer. Figure 5 shows the histogram of that position for three cases. In all cases we have $l_p = 15\sigma$. Furthermore, we choose: (a) $N = 60$, $R = 1.3\sigma$, and $k^a = 5$, (b) $N = 100$, $R = 2\sigma$, $k^a = 4$, and (c) $N = 100$, $R = 2\sigma$, and $k^a = 7$. Case (a) corresponds to the parameter set already studied in Figure 4 where we found $N_{loop} = 30$ as the typical loop length. In Figure 5a, one observes that most loops have their center between monomer numbers 20 to 40, i.e., in the middle of the chain. This is consistent with the typical loop sizes: Since a loop can exist only between two adsorbed chain portions, the loop cannot be situated closer to the termini than $N_{loop}/2$.

The two cases with a longer chain of $N = 100$ monomers, case (b) and (c) in Figure 5, show a much broader distribution of loop positions. In the case (b) with small adsorption strength, $k^a = 4$, the distribution has one broad maximum around the centered loop. Remarkably, this maximum divides into three peaks around 1/4, 1/2, 3/4 when the adsorption energy is increased toward the value $k^a = 7$. This is reminiscent of the peaks observed for *wrapped* complexes that occur at high adsorption strength, cf. Figure 3. There we argued that the peaks are mostly of enthalpic origin, namely that one-tail configurations allow more monomers to adsorb on the ball. Presumably we have here a similar situation. The outer peaks might again reflect one-tail complexes, with the inner peak corresponding to special chain conformations that allow the adsorption of an additional monomer. A further analysis of this effect would require a detailed study of the possible geometries of the wrapping/loop structure that is beyond the scope of the current work.

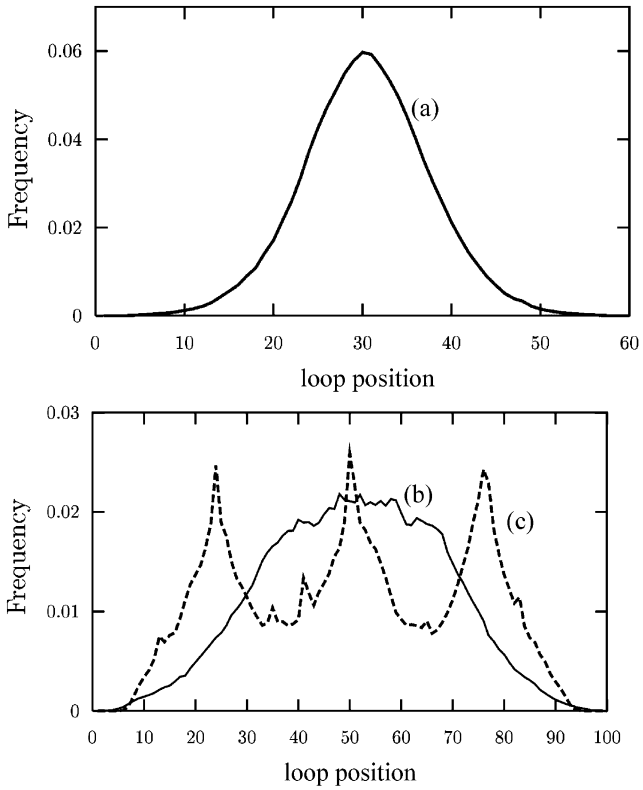

Figure 5. Histograms of the central loop monomer number for $k^b = 15\sigma$ in three cases: (a) $N = 60$, $R = 1.3\sigma$, $k^a = 5$, (b) $N = 100$, $R = 2\sigma$, $k^a = 4$, and (c) $N = 100$, $R = 2\sigma$, $k^a = 7$.

V. Dynamic Properties: Chain Closed into a Ring

In this section we study the diffusion of the sphere *along* the chain. The general idea is to extract the corresponding diffusion constant from the mean-squared displacement (MSD) of the sphere position. We want to study whether the sphere can "slide" along the chain even in the absence of loop defects, i.e., when the complex is in a state as examined in section III.

To measure the diffusion constant there are two major obstacles to overcome. (*i*) As emphasized in section IV, there is a nonvanishing probability of loops on the complex. As discussed in ref 23, such a loop can form on one side of the wrapped chain portion and might then diffuse around the complex to the other end. There the length that is stored in the loop is released, leading to a corresponding repositioning step of the sphere; the resulting repositioning dynamics is then superdiffusive.[23] (*ii*) The chain has a finite length. As a consequence, the MSD of the sphere diffusion along the chain saturates when a value on the order of $(\sigma N)^2$ is reached.

To circumvent these problems we choose the following strategy. (*i*) We discard all simulation runs during which a loop has been created. That way we make sure that we only pick the sphere mobility in the loop-free state of the complex. (*ii*) We close the chain into a ring. We keep track of the number of times the sphere travels around the chain. In this way the MSD vs. time t shows a linear behavior, with the slope being related to the diffusion coefficient, and there is no saturation. Two example configurations of complexes with such a closed chain are depicted in Figure 1d and e, the latter example being a structure with a loop defect, i.e., a structure that we would discard in our simulation.

Figure 6 shows four examples of the MSD, $\langle (n(t) - n(0))^2 \rangle$, of the particle as a function of time. Here and in the following both the chain and the sphere are free to move. In all four cases

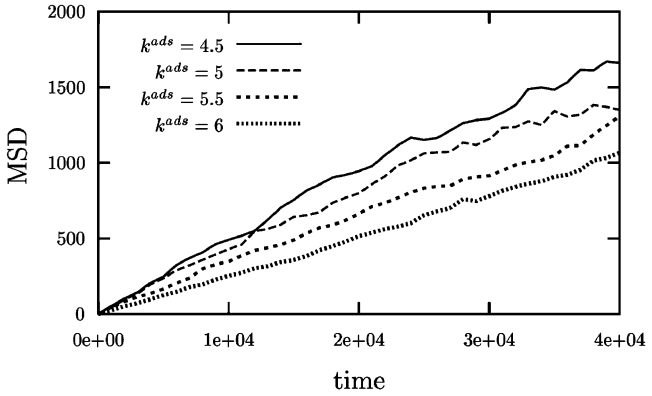

Figure 6. MSD of the ball along the chain (in units of σ^2) against time (in units of τ_{LJ}) as a function of the absorption energy for four different values of k^a (as indicated in the figure). The other parameters are chosen as follows: $k^b = 15$, $N = 86$, and $R = 1.3\sigma$. From the slope of the curves we extracted the following diffusion constants (in units of σ^2/τ_{LJ}): $D = 0.021$ for $k^a = 4.5$, $D = 0.018$ for $k^a = 5$, $D = 0.015$ for $k^a = 5.5$, and $D = 0.013$ for $k^a = 6$.

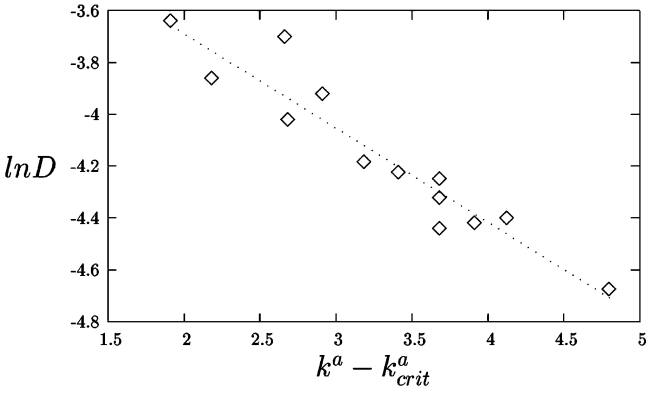

Figure 7. Diffusion constant D (in units of σ^2/τ_{LJ}) of the sphere motion along the chain as a function of $k^a - k^a_{crit}$. The system properties for all data points are listed in Table 1.

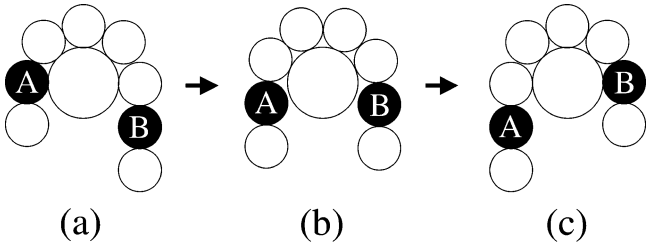

Figure 8. Chain sliding as a possible mechanism underlying the repositioning. A repositioning step by one monomer from state (a) (with monomer A attached and monomer B detached) to state (c) (with monomer B attached and monomer A detached) goes via an intermediate (b). In this state, both black monomers are desorbed but still feel the attractive potential from the ball (see text).

we chose $N = 86$, $R = 1.3\sigma$, and $k^b = 15$. The adsorption constant k^a varies as indicated in the figure. From the MSD the diffusion constant D of the relative diffusion of the sphere along the chain can be extracted via the relation $\langle (n(t) - n_0))^2 \rangle \sigma^2 = 2Dt$. As can be seen, the diffusion constant (in units of σ^2/τ_{LJ}) varies monotonically with k^a, going from $D = 0.021$ for $k^a = 4.5$ to $D = 0.013$ for $k^a = 6$ (cf. also the first four columns of Table 1).

To determine how the diffusion coefficient depends on the properties of the system, i.e., on the adsorption energy k^a, the persistence length $l_p = \sigma k^b$, the ball radius R, and the chain length N, we performed a series of simulation runs where we varied these quantities as summarized in Table 1. The general trends are as follows. The diffusion constant goes up with decreasing values of k^a and R and with increasing value of k^b. There is only a weak dependence of D on the chain length N.

These general trends go in the following direction: the harder it is to desorb a monomer from the surface of the sphere at one end of the wrapped portion, the slower is the diffusion of the chain. The cost to unwrap a monomer has been calculated in eq 8 to be $k^a - k^a_{crit}$. A repositioning step of the ball is typically associated with the desorption of a monomer at one end and the subsequent adsorption on the other end. The desorption step is thermally activated and should have a typical rate proportional to $\exp(-(k^a - k^a_{crit}))$. We therefore expect the diffusion constant to be proportional to this factor. We check this in Figure 7 by plotting the diffusion constant against $k^a - k^a_{crit}$ in a semilogarithmic plot using all the data from Table 1. The data points indeed collapse roughly onto a line, indicating that the monomer desorption rate governs to a large extent the mobility of the sphere along the chain.

We note, however, that the dotted line in Figure 7 has a slope smaller than one, namely the line is given by $-\mu(k^a - k^a_{crit})$, with $\mu = 0.36$. This indicates that the desorption event is less costly than $(k^a - k^a_{crit})$, which is possible only when another monomer is adsorbed at the same time. This points toward a sliding of the chain along the ball where the desorption of a monomer is compensated by the simultaneous adsorption of a monomer at the other end of the wrapped portion. The transition state and its energy depend on microscopic details and are difficult to calculate. One could imagine that this state corresponds to a symmetric configuration in which one monomer is halfway desorbed and the other halfway adsorbed, cf. Figure 8. This state has indeed an energy barrier that is smaller than $(k^a - k^a_{crit})$. For example, for $k^a = 5$, $k^b = 15$, $R = 1.3\sigma$, and $\alpha = 6$ one finds a desorption energy $k^a - k^a_{crit} \approx 2.7$, whereas the transition state during sliding is just $\approx 1 k_B T$ above the wrapped state. The exact dependence on all properties is, however, complicated and cannot simply be taken into account via the prefactor μ. This means that the linear dependence indicated by the dotted line in Figure 7 can only be considered as giving the general trend; a perfect collapse of all the data points on that line should not be expected.

We note an additional complication associated with varying the ball size R. To a first approximation the diffusion constant should show a dependence $D \propto \xi_s^{-1} \exp(-\mu(k^a - k^a_{crit})$ where R enters through k^a_{crit}, cf. eq 8, but also through the friction constant of the sphere, $\xi_s = 2\xi R/\sigma$. This might, for instance, explain why the data point at $\ln D \approx -3.7$ and $k^a - k^a_{crit} \approx 2.6$ is located above the line: this point corresponds to the smallest sphere ($R = \sigma$), and hence the one that shows the highest

TABLE 1: Diffusion Constants (in units of σ^2/τ_{LJ}) Measured for Different Sets of k^a, k^b, R (in units of σ), and N

k^a	4.5	5	5.5	6	6	6	5	6	6.5	7	6	6	6
k^b	15	15	15	15	15	15	20	20	20	20	15	15	15
R	1.3	1.3	1.3	1.3	1.3	1.3	1.3	1.3	1.3	1.3	1	1.5	2
N	86	86	86	86	70	100	86	86	86	86	86	86	86
$k^a - k^a_{crit}$	2.19	2.69	3.19	3.69	3.69	3.69	1.91	2.91	3.91	2.91	2.67	4.13	4.8
D	0.021	0.018	0.015	0.013	0.013	0.014	0.026	0.020	0.015	0.012	0.025	0.012	0.009

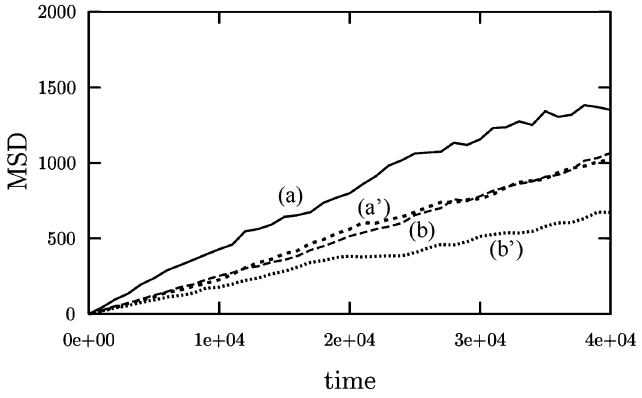

Figure 9. MSD (in units of σ^2) of the relative diffusion between chain and sphere as a function of time (in units of τ_{LJ}). Compared here are the cases (a,b) where the sphere is free to move and (a′,b′) where it is fixed in space. In all runs we set $N = 86$, $R = 1.3\sigma$, and $k^b = 15$. For both cases we depict curves for two adsorption energies: (a,a′) $k^a = 5$ and (b,b′) $k^a = 6$. For the mobile sphere we find (a) $D = 0.018$ and (b) $D = 0.013$, respectively. If the sphere is fixed, the relative diffusion between the ball and the chain is considerably smaller, namely (a′) $D = 0.013$ and (b′) $D = 0.008$, respectively.

mobility. How strongly the sphere mobility influences the diffusion constant of the complexed sphere along the chain becomes especially apparent in Figure 9. Depicted is the MSD as a function of t for the case of a mobile sphere (as used so far throughout the present section) and of a sphere that is fixed in space. In all cases we choose $N = 86$, $R = 1.3\sigma$, and $k^b = 15$. Whereas we found (a) $D = 0.018$ for $k^a = 5$ and (b) $D = 0.013$ for $k^a = 6$ for the free sphere, the repositioning is considerably reduced for the sphere fixed in space, namely (a′) $D = 0.013$ for $k^a = 5$ and (b′) $D = 0.008$ for $k^a = 6$.

VI. Conclusion and Discussion

We treat a simple case of a colloidal particle "wrapped" by a polymer chain, using Brownian molecular dynamics simulation to investigate both the static properties of this system and the diffusional dynamics of the particle changing its position with respect to the chain without becoming unwrapped from it.

First we establish the dependence of the wrapped chain length on absorption energy and chain persistence length and obtain the distribution of wrapped-chain positions. This distribution is necessarily symmetric about the chain center, and we find that it has two peaks favoring the ends of the chain, with this preference becoming more pronounced for shorter unwrapped positions ("arms"). We argue that this is an energetic effect related to a small difference in the average number of adsorbed monomers: a complex with a single tail has slightly more space for adsorbing monomers than a two-tail complex.

We also made an analysis of the loop formation statistics. Our simulations confirm that the loop has a preferred size of order two times the chain persistence length, independent of overall chain length and absorption energy. Furthermore, the distribution of loop positions favors the center of the chain.

Then we focus on the diffusional dynamics of the particle as it repositions itself along the chain that wraps it. We calculate the mean square displacement of the central monomer of the wrapped portion of the chain, determine how the corresponding diffusion coefficient depends on system properties, i.e., radius of the particle, chain persistence length, overall contour chain length, and absorption energy. From these dependencies we conclude that the repositional dynamics is mainly governed by detachment/attachment events of individual monomers at the ends of the wrapped portion. This is related to the fact that the diffusion constant is roughly proportional to $\exp(-\mu(k^a - k^a_{crit}))$ with $k^a - k^a_{crit}$ being the effective desorption energy of a single monomer. The fact that the prefactor is smaller than one (we find $\mu \approx 0.4$) shows that the barrier against repositioning is somewhat reduced. We believe that this reflects a simultaneous desorption/adsorption event that results from a simple sliding of the chain along its wrapped portion where the desorption of a monomer at one end is balanced by the adsorption of a monomer at the other end.

We note here that this repositioning via simple sliding is possible only because the sphere is attracting monomers homogeneously all over its surface. If instead the attraction were localized at small binding patches on the sphere surface, repositioning could occur only via different mechanisms. Repositioning of nucleosomes along DNA is a prominent example of localized adsorption sites.[29−31] In nucleosomes, DNA is wrapped in 1 and 3/4 turns around a cylindrical octamer of histone proteins. The interaction between DNA and the octamer is localized at 14 binding sites where the minor groove of the DNA faces the octamer surface.[32] Each binding site has an adsorption energy of roughly $6k_BT$.[3] Simple sliding, as observed in our above ball−chain model, would involve the simultaneous breakage of all 14 binding sites, which is energetically too costly. It is therefore believed that repositioning takes place via intermediate states that constitute a smaller energy barrier. Two possible mechanism are repositioning via loop- and twist defects.[3,24] Recent experiments[31] indicate that it is the latter mechanism that most likely underlies nucleosome repositioning: Base-pair twist defects (one missing or one extra basepair) enter the wrapped portion of the DNA and diffuse through the chain to the other end where the extra (or missing) length is released, effectively leading to the repositioning of the nucleosome.[25,26] This results in an overall corkscrew motion of the cylinder relative to the DNA chain.

In view of these experiments it would be interesting to study, along lines similar to the present paper, ball−chain complexes with structured binding patches on the ball surface that forbid a simple sliding of the complexed chain and to see whether sphere repositioning still occurs and by what mechanism.

Acknowledgment. We thank D. Reguera-López, Kun-Chun Lee, J. T. Kindt, and M. Deserno for valuable discussions. This work was supported by CONACyT-Mexico under Grant SEP-2003-C02-43780, UC-MEXUS and the NSF under Grant No. DMR-9708646.

References and Notes

(1) Vincent, B. *Adv. Colloid Interface Sci.* **1974**, *4*, 193.
(2) McQuigg, D. W.; Kaplan, J. I.; Dubin, P. L. *J. Phys. Chem.* **1992**, *96*, 1973 and references therein
(3) Schiessel, H. *J. Phys.: Condens. Matter* **2003**, *15*, R699.
(4) Skepö, M.; Linse, P. *Macromolecules* **2003**, *36*, 508.
(5) Pincus, P. A.; Sandroff, C. J.; Witten, T. A. *J. Phys. (Paris)* **1984**, *45*, 725.
(6) Marky, N. L.; Manning, G. S. *Biopolymers* **1991**, *31*, 1543.
(7) Park, S. Y.; Bruinsma, R. F.; Gelbart, W. M. *Europhys. Lett.* **1999**, *46*, 454.
(8) Mateescu, E. M.; Jeppesen, C.; Pincus, P. *Europhys. Lett.* **1999**, *46*, 493.
(9) Gurovitch, E.; Sens, P. *Phys. Rev. Lett.* **1999**, *82*, 339.
(10) Nguyen, T. T.; Shklovskii, B. I. *Physica A* **2001**, *293*, 324.
(11) Schiessel, H.; Bruinsma, R. F.; Gelbart, W. M. *J. Chem. Phys.* **2001**, *115*, 7245.
(12) Stoll, S.; Chodanowski, P. *Macromolecules* **2002**, *35*, 9556.
(13) Netz, R. R.; Joanny, J.-F. *Macromolecules* **1999**, *32*, 9026.
(14) Kunze, K.-K.; Netz, R. R. *Phys. Rev. Lett.* **2000**, *85*, 4389.
(15) Wallin, T.; Linse, P. *Langmuir* **1996**, *12*, 305.
(16) Schiessel, H.; Rudnick, J.; Bruinsma, R.; Gelbart, W. M. *Europhys. Lett.* **2000**, *51*, 237.

(17) Akinchina, A.; Linse, P. *Macromolecules* **2002**, *35*, 5183.
(18) Schiessel, H. *Macromolecules* **2003**, *36*, 3424.
(19) Akinchina, A.; Linse, P. *J. Phys. Chem. B* **2003**, *107*, 8011.
(20) Laguecir, A.; Stoll, S.; Kirton, G.; Dubin, P. L. *J. Phys. Chem. B* **2003**, *107*, 8056.
(21) Schiessel, H.; Widom, J.; Bruinsma, R. F.; Gelbart, W. M. *Phys. Rev. Lett.* **2001**, *86*, 4414. Schiessel, H.; Widom, J.; Bruinsma, R. F.; Gelbart, W. M. *Phys. Rev. Lett.* **2002**, *88*, 129902.
(22) Sakaue, T.; Yoshikawa, K.; Yoshimura, S. H.; Takeyasu, K. *Phys. Rev. Lett.* **2001**, *87*, 078105.
(23) Kulić, I. M.; Schiessel, H. *Biophys. J.* **2003**, *84*, 3197.
(24) Flaus, A.; Owen-Hughes, T. *Biopolymers* **2003**, *68*, 563.
(25) Kulić, I. M.; Schiessel, H. *Phys. Rev. Lett.* **2003**, *91*, 148103.
(26) Mohammad-Rafiee, F.; Kulić, I. M.; Schiessel, H. *J. Mol. Biol.* **2004**, *344*, 47.
(27) Chuang, J.; Kantor, Y.; Kardar M. *Phys. Rev. Lett.* **2001**, *65*, 011802.
(28) Yamakawa, H.; Stockmayer, W. *J. Chem. Phys.* **1972**, *57*, 2843.
(29) Pennings, S.; Meersseman, G.; Bradbury, E. M. *J. Mol. Biol.* **1991**, *220*, 101.
(30) Flaus, A.; Richmond, T. J. *J. Mol. Biol.* **1998**, *275*, 427.
(31) Gottesfeld, J. M.; Belitsky, J. M.; Melander, C.; Dervan, P. B.; Luger, K. *J. Mol. Biol.* **2002**, *321*, 249.
(32) Luger, K.; Mäder, A. W.; Richmond, R. K.; Sargent, D. F.; Richmond, T. J. *Nature* **1997**, *389*, 251.